PERGAMON

International Journal of Heat and Mass Transfer 45 (2002) 3961–3971

International Journal of HEAT and MASS TRANSFER

www.elsevier.com/locate/ijhmt

An experimental study of high Weber number impact of methoxy-nonafluorobutane $C_4F_9OCH_3$ (HFE-7100) and *n*-heptane droplets on a heated solid surface ☆

Samuel L. Manzello *,[1], Jiann C. Yang

Building and Fire Research Laboratory, National Institute of Standards and Technology, 100 Bureau Drive, Stop 8662, Building 224, A361, Gaithersburg, MD 20899, USA

Received 10 August 2001; received in revised form 1 March 2002

Abstract

An experimental study is presented for methoxy-nonafluorobutane ($C_4F_9OCH_3$, HFE-7100) droplet impingement on a heated stainless steel surface. The impaction process was recorded using a high-speed digital camera at 1000 frames per second. The initial droplet diameter was fixed at 1.7 ± 0.1 mm, and all experiments were performed in atmospheric air. The impact velocity was fixed at 2.0 m/s thus defining an impact Weber number of 750. The temperature of the stainless steel surface was varied from 20 to 300 °C, above the Leidenfrost temperature of HFE-7100. Experiments were also performed using *n*-heptane to investigate whether the collision dynamics were similar if the impact Weber number was matched to HFE-7100 and collision considered within the same boiling regimes as HFE-7100. While the collision dynamics were qualitatively similar, the evolution of liquid film diameter with time was different. Existing models used to describe the evolution of liquid film diameter with time were found to be inadequate to describe HFE-7100 and *n*-heptane impact. Published by Elsevier Science Ltd.

Keywords: Droplet; Impact; Heated surface

1. Introduction

Due to the ban of Halon 1301 under the Montréal Protocol, new liquid fire suppressants have been proposed as possible alternatives to Halon 1301 in certain fires [1]. These systems contain a liquid fire suppressant (typically under high pressure) that is subsequently atomized into droplets traveling with high velocities. Downie et al. [2] have reported that in the case of water mist fire suppression systems, a large fraction of the impinging droplets do not penetrate the fire since the droplet momentum is so small that the droplets can be directed away from the rising fire plume. King et al. [1] suggest that these deflected droplets impinge upon heated surfaces near the fire and ultimately evaporate. These droplets can still act to suppress the fire since evaporating droplets provide surface cooling of nearby heated surfaces and the vapor from these evaporating droplets may ultimately be entrained into the fire [1]. Therefore, understanding high velocity droplet impingement upon heated surfaces within close proximity to the fire can have implications upon fire suppression.

Under practical conditions, the dispersion of the liquid agent results in the generation of numerous droplets that can be difficult to study systematically. A simpler approach must be adopted to understand the influence of droplet impingement on a heated surface. One such approach is the study of single droplet impingement upon heated surfaces. Single droplet studies can be used to understand the transient heat transfer characteristics which are required in order to predict the global heat transfer characteristics of an entire spray [3].

☆ Official contribution of the National Institute of Standards and Technology not subject to copyright in the United States of America.

* Corresponding author. Tel.: +1-301-975-6891; fax: +1-301-975-4052.

E-mail address: samuel.manzello@nist.gov (S.L. Manzello).

[1] NRC Post-Doctoral Fellow.

0017-9310/02/$ - see front matter Published by Elsevier Science Ltd.
PII: S0017-9310(02)00103-5

Nomenclature

c	specific heat
D_f	liquid film diameter
D	initial droplet diameter
k	thermal conductivity
Re	Reynolds number
t	time
V	impact velocity
We	Weber number
Greek symbols	
μ	dynamic viscosity
v	kinematic viscosity
ρ	density
σ	surface tension
τ	normalized time (tV/D)
Subscripts	
c	critical
L	liquid
Leid	Leidenfrost
max	maximum

Liquid droplet interaction with a surface has been studied for more than 100 years [4–6]. The characteristics of the droplet/surface interactions depend upon the properties of the droplet, the impacted surface, impact velocity, geometry, and the medium (liquid, gas, dispersion) through which the droplet traverses prior to impact [7]. Despite many investigations [8–19], the complicated fluid mechanic processes associated with liquid droplet/surface interaction is not yet well understood.

The impact of a liquid droplet with a solid surface can result in droplet spread, splash, or rebound [7]. Whether a droplet will spread, splash, or rebound is dependent upon the impact energy, surface temperature, and surface roughness [3,9,14]. The parameter used to quantify the impact energy is the Weber number, [7]

$$We = \frac{\rho V^2 D}{\sigma} \tag{1}$$

where ρ is the liquid density, V is the impact velocity of the droplet, D is the initial droplet diameter, and σ is the liquid phase surface tension. The heating of the solid surface can influence the droplet collision process as well [14]. For a droplet impinging upon a heated surface, droplet evaporation occurs as the droplet approaches the surface. For temperatures greater than the Leidenfrost temperature, rapid vapor generation creates large flow disturbances that breakup the spreading liquid film [3].

Wachters and Westerling [9] investigated water droplet impact on a heated surface. The water droplets were fixed around 2 mm and a polished gold surface maintained at 400 °C was used. From these experiments, three distinct impact regions were identified. Each region was observed to be a function of the impact Weber number, defined using Eq. (1). For an impact Weber number greater than 80, the droplet was observed to form a thin, spreading liquid film upon impact. This film ultimately disintegrated into many tiny droplets. With an impact Weber number between 30 and 80, the droplet never disintegrated upon impact. Rather, the droplet disintegrated after it was observed to rise above the surface. When the impact Weber number was reduced below 30, the droplet never broke up. The droplet impacted the surface and subsequently lifted off the surface after impact without breakup.

Chandra and Avedisian [14] have studied the collision dynamics of a liquid droplet on a heated solid stainless steel surface. In these experiments, *n*-heptane droplets of 1.5 mm initial diameter were used and the surface temperature was varied from 24 to 250 °C. The impact velocity was fixed at 0.93 m/s, thus defining an impact Weber number of 43. The single shot photographic technique employed provided clear, vivid pictures of the droplet impact process. The droplet spreading rate and contact angle were measured as a function of surface temperature for the impinging droplets. It was reported that the droplet spreading rate was independent of temperature directly after impact. In addition, the contact angle was observed to increase with increasing temperature.

Ko and Chung [16] investigated *n*-decane droplet impact upon inclined heated surfaces. The droplet size and wall temperature were varied from 300 to 500 μm, and 220 to 300 °C, respectively. The impinging velocity of the droplets was varied from 0.6 to 1.0 m/s. In addition, the surface was inclined from 45 to 90°. Impact at 90° was defined as impact normal to the surface. They were interested in droplet breakup resulting from impact on the heated surfaces and defined the droplet breakup probability as the ratio of the number of droplets observed to breakup to the total number of droplets impinging upon the heated surface. Further, a 50% breakup probability was defined as the criterion necessary for breakup. It was reported that at 50% probability of droplet breakup, the impinging velocity decreased with an increase in droplet diameter. Additionally, for an impinging angle of 80°, the impinging

velocity was lowest for a given wall temperature, defining an optimum impinging angle for the droplet breakup.

Bernardin et al. [3] performed a comprehensive study of water droplet impingement on a heated aluminum surface. The impinging droplet diameter was fixed at 3.0 mm and the impact velocity was set at 0.70, 1.21 or 2.34 m/s. This resulted in impact Weber numbers of 20, 60, and 220. The temperature of the heated surface was also varied from 100 to 280 °C. The impact dynamics were imaged using high-speed photography at 1000 frames/s in conjunction with single flash photography. Regime maps were generated as a function of temperature for the three different impact Weber numbers considered. It was observed that the impact Weber number greatly influenced the spreading characteristics and the stability of the droplet upon impact. The liquid film radius was also measured as a function of temperature and impact velocity and compared to water droplet impingement correlations in the literature. The correlations provided poor agreement to the measured liquid film radius.

Based upon review of the literature, significant work has been performed for water droplet impingement on heated surfaces. In addition, hydrocarbon impact (e.g. *n*-heptane) has been studied extensively as well. While most studies have focused on low Weber number impact, high Weber number impact is important for fire suppression applications.

An effort is underway at the National Institute of Standards and Technology (NIST) to study droplet impact on heated surfaces from a fire suppression perspective. An experimental study was performed for methoxy-nonafluorobutane, $C_4F_9OCH_3$ (HFE-7100) droplet impingement on a heated solid surface. HFE-7100 was selected as the fluid in this study because it is currently being screened as a potential fire suppressant [20]. Since HFE-7100 has a low surface tension (see Table 1), high Weber number impact can be achieved with a relatively low impact velocity. The evaporation time was obtained as a function of surface temperature for HFE-7100, and droplet impact was studied throughout this temperature range. Specifically, the collision dynamics were considered within the nucleate boiling, transition boiling, and film boiling regimes. In addition to HFE-7100, *n*-heptane was used as a calibration fluid for the droplet impingement experiments.

Table 1
Selected thermophysical properties at 25 °C

Fluid	Density (ρ) kg/m^3	Dynamic viscosity (μ) Ns/m^2	Surface tension (σ) N/m	Normal boiling point (°C)
n-Heptane	679	3.9×10^{-4}	0.0202	98.4
HFE-7100	1500	6.1×10^{-4}	0.0136	61

n-Heptane was selected because it has been studied extensively for solid surface impact thus affording comparison to the work in the literature, and to determine whether similar impact dynamics could be observed for both HFE-7100 and *n*-heptane by matching the impact Weber number and surface temperatures within the nucleate boiling, transition boiling, and film boiling regimes for both fluids.

2. Experimental description

Fig. 1 is a schematic of the experimental setup. The HFE-7100 and *n*-heptane droplets were generated using a syringe pump programmed to dispense the liquid at a rate of 0.001 ml/s. The droplet was formed at the tip of the needle (22 gauge) and detached off the syringe under its own weight. To measure the droplet evaporation lifetime, droplets were gently placed on a rectangular stainless steel surface (SS 304), 3 cm wide, 5 cm long, and 0.5 cm thick. The stainless steel surface was polished based upon recommendations of previous work [14]. Sand paper (600 grit) was first used to polish the surface with subsequent application of metal polish to create a mirror finish. Surface heating was accomplished using a copper block with two miniature cartridge heaters embedded within it. The surface temperature was measured using a thermocouple embedded within the stainless steel surface. The location of the thermocouple was centered within the block and inserted 1 mm below the surface. It must be noted that all temperatures reported in this study correspond to those measured in solid. The surface temperature was controlled within ± 1 °C using a temperature controller. A CCD camera (with a framing rate of 30 frames per second) was used to measure the droplet evaporation time.

Droplet impingement dynamics were imaged using a Kodak [2] EktaPro 1000 HRC Digital High Speed Camera at 1000 frames per second with shutter speed set to 50 μs. The Kodak High Speed Camera was fitted with a Nikon 60 mm microlens to obtain the required spatial resolution to capture droplet impingement. The camera was aligned at an angle $\theta = 33°$ with respect to the horizontal. The entire process was back-lit using one 410 W light source (see Fig. 1). A ground glass diffuser was placed in front of the light source to provide uniform illumination for the camera.

The impact velocity was measured by tracking the location of the droplet centroid 2 ms prior to impact using an image processing software. The initial droplet diameter was determined 2 ms prior to impact. The

[2] Certain commercial equipment are identified in this paper in order to accurately describe the experimental procedure. This in no way implies recommendation by NIST.

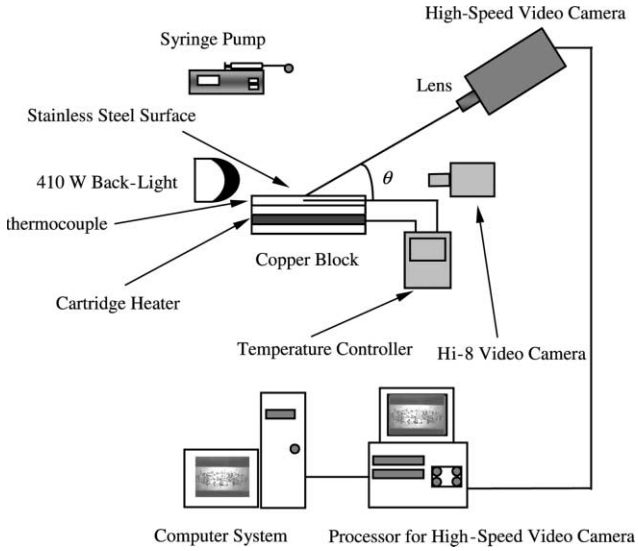

Fig. 1. Schematic of experimental setup.

image processing software was used to threshold the droplet from the background and the diameter of the droplet was measured both in the horizontal and vertical direction. The difference in the diameter measured in the vertical and horizontal direction was at most 0.3 mm. The droplet diameter was defined as the average of the two measurements. The computer system was used to store the digital images for subsequent analysis.

3. Results and discussion

Fig. 2 displays the evaporation lifetime as a function of surface temperature for an HFE-7100 droplet with initial diameter of 1.7 ± 0.1 mm. The evaporation lifetime as a function of surface temperature can be used to delineate different heat transfer regimes, thus providing a mechanism to better understand the influence of surface temperature on droplet collision dynamics [21]. The total evaporation lifetime was defined as the time the droplet disappeared from the surface minus the time the droplet was placed upon the surface. At each temperature three sequential experiments were performed and the evaporation time at each temperature represents the average of the three runs with the error bars representing the standard deviation of each measurement (mean $\pm$ s.d.). Since the droplet evaporation lifetime as a function of surface temperature was determined by gently placing the droplet on the heated surface, it is assumed that the two points that define the curve, the departure for nucleate boiling and the Leidenfrost temperature, do change significantly as the droplet velocity was increased. Bernardin et al. [3] observed that the temperature for departure for nucleate boiling and the

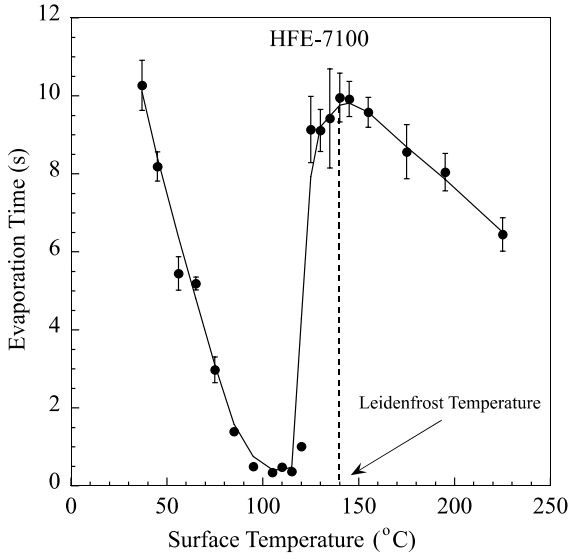

Fig. 2. Measured evaporation lifetime for HFE-7100 as a function of surface temperature.

Leidenfrost point were insensitive to droplet impact velocity (upto 2.34 m/s) and droplet impingement frequency.

For a surface temperature less than the boiling point of HFE-7100, droplet impact should result in wetting of the impacted surface without boiling. From Fig. 2, the minimum evaporation time occurs at 105 °C, which corresponds to the surface temperature where departure from nucleate boiling occurs. Nucleate boiling is expected for surface temperatures from the normal boiling

point, 61 °C, up to 105 °C. As the surface temperature is increased beyond 105 °C, the Leidenfrost point is approached (i.e. temperature where evaporation time reaches a local maximum). The Leidenfrost temperature for HFE-7100 was 140 °C. Transition boiling will occur for HFE-7100 from 105 to 140 °C. Beyond the Leidenfrost point, the evaporation rate decreases monotonically with surface temperature. The regime is known as film boiling.

The correlation from Baumeister and Simon [22] was used to estimate the Leidenfrost temperature:

$$T_{\text{Leid}} = T_{\text{L}} + \frac{\frac{27}{32}T_{\text{C}} - T_{\text{L}}}{\exp(0.00175\beta)\text{erf}c(0.042\sqrt{\beta})} \tag{2}$$

where T_{L} is the liquid temperature, T_{c} the critical temperature of the liquid, and $\beta = (k\rho c)^{-1}$ where k is the thermal conductivity, ρ the density, and c the heat capacity of the impacted surface. Based on this correlation, the Leidenfrost temperature was calculated to be 150 °C for HFE-7100. This value agreed quite well with the measured value of 140 °C for HFE-7100.

Fig. 3 displays time elapsed images of HFE-7100 droplet impingement at $We = 750$ upon a stainless steel surface for surface temperatures of 20, 61, 105, 140 and 300 °C, respectively. Several experiments were performed at each temperature. The collision dynamics were repeatable for each case. Since each experiment displayed the same qualitative trends, results of three consecutive experiments were used for data analysis. The temporal resolution of the photographs was limited to 1 ms, the framing rate of the imaging system. The impact Weber number ($We = 750$) was defined using Eq. (1). At 1 ms after impact, the droplet was observed to flatten. The flattening of the droplet is a consequence of high pressure induced after impact. The pressure is relieved by the liquid droplet stretching radially outward upon impact [14].

For HFE-7100 impact on a solid surface at the normal boiling temperature, 61 °C, cellular structures begin to appear within the liquid film 4 ms after impact. Cellular structures within the liquid film were also observed by Chandra and Avedisian [14] for *n*-heptane droplets impacting on a heated solid surface. It is speculated that cellular structures arise due to surface tension gradients within the liquid film resulting from the heat transfer from the hot surface.

The collision dynamics at departure from nucleate boiling (105 °C) were dramatically different than at the normal boiling point, 61 °C. Immediately after impact, the droplet was observed to disintegrate into many small droplets. At 5 ms after impact, the initial droplet was completely shattered.

For droplet impact at 140 °C, the Leidenfrost temperature of HFE-7100, the droplet was observed to flatten into a large disk immediately after impact. Small droplets were ejected from the periphery of this disk. At 5 ms after impact, the small liquid film present within the disk was observed to violently breakup into several droplets. The collision dynamics at 300 °C (film boiling) were qualitatively similar to the impact at 140 °C.

The liquid film diameter was measured as a function of time for HFE-7100 impact and is shown in Fig. 4a. The liquid film diameter was measured for three experiments performed at each temperature. The diameter was defined as the average of the three measurements with the error bars representing the standard deviation. This diameter was measured upto the time of droplet breakup. From this curve (see Fig. 4a), three distinct regions can be observed. For surface temperatures within the film evaporation regime to the nucleate boiling regime, the liquid film diameter increased with time up to 3 ms after impact. The lowest temperature, 20 °C, resulted in the largest diameter. A transition occurred at departure from nucleate boiling (105 °C). The liquid film diameter increased to a value of 8 mm within 1 ms. However, as observed in Fig. 3, the liquid film became unstable, and as a result the liquid film diameter could no longer be measured. The third distinct regime in Fig. 4a occurred for surface temperature within the film boiling regime. Here, the liquid film diameter was larger than in the film evaporation and nucleate boiling regimes. The liquid film diameter increased with time for all temperatures considered within the film boiling regime and became unstable 3–4 ms after impact.

A comparison of the evolution of liquid film diameter with time was made with existing models of droplet spread on a heated surface. At present, no models exist in the literature for HFE-7100. Consequently, comparisons were performed for models validated for water impact.

Within the film boiling regime, Bolle and Moureau [23] developed a correlation valid for determining the evolution of liquid film diameter D_{f} as a function of time. The equation is given as:

$$\frac{D_{\text{f}}}{D} = 1.67\left[3.1\tau - \tau^2\right] \tag{3}$$

where $\tau = t/t^+ = tV/D$, t is time, and V is impact velocity. This correlation was obtained based on water droplet impingement and was valid for time, $0.2t^+ \leqslant t \leqslant (1.2\text{–}1.5)t^+$. Another correlation suggested to describe droplet spread within the film boiling regime is that of Shi and Chen [24]. The correlation has the following form:

$$D_{\text{f}}(t) = 1.6V\left[t - \frac{6.8\sigma}{\rho D^3}V^{0.25}t^{2.95}\right] + D \tag{4}$$

Fig. 4b displays the measured spread diameter within the film boiling regime in conjunction with model predictions. The Bolle and Moureau [23] correlation does a

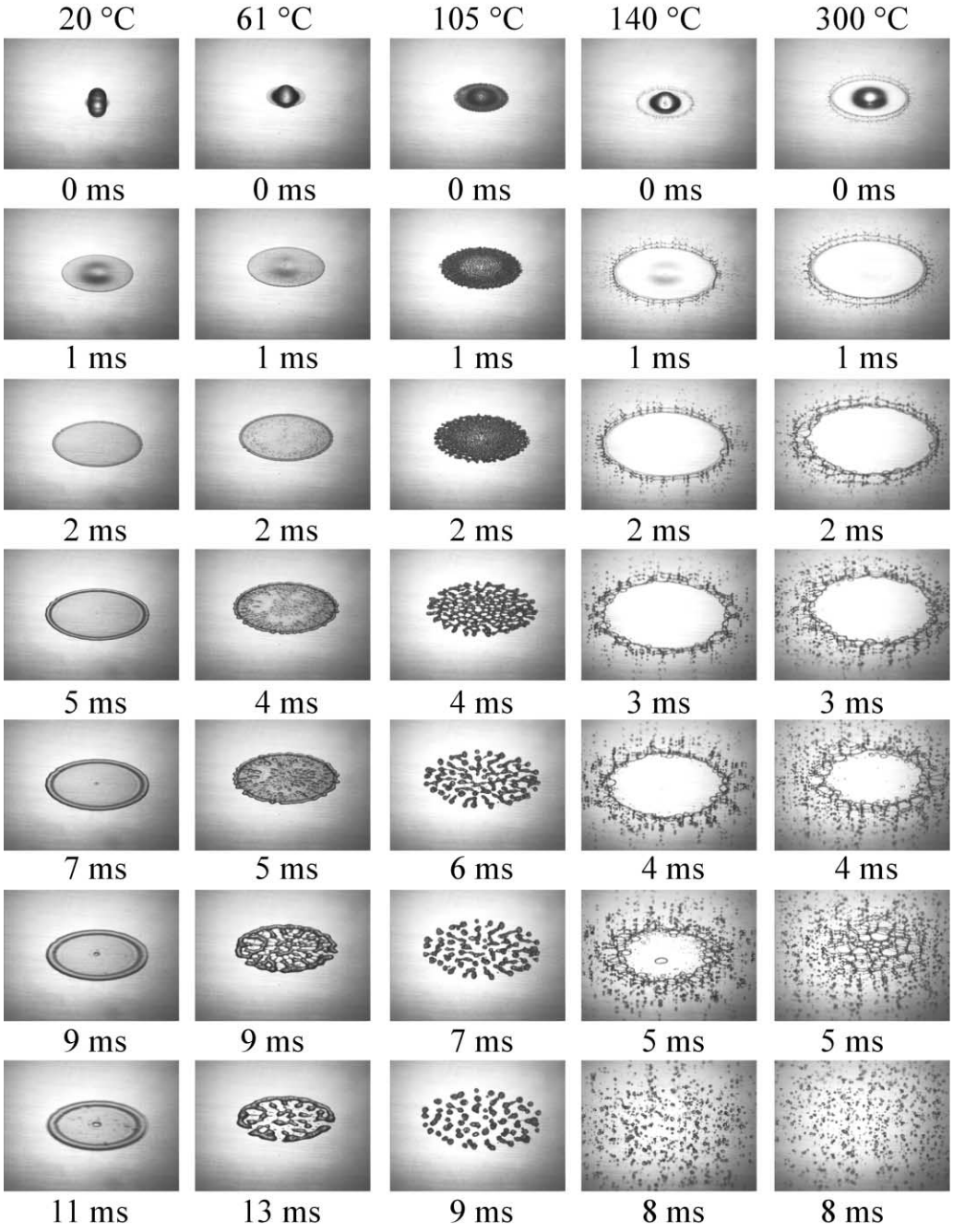

Fig. 3. Time elapsed images of HFE-7100 droplet impingement upon a stainless steel surface at $We = 750$.

poor job of predicting the evolution of liquid film diameter. The liquid film diameter was under predicted as was the time to reach the maximum liquid film diameter. This is not surprising since the correlation was based upon water impact, and as noted by Bolle and Moureau [23] that this correlation is most likely not applicable to other fluids. The correlation of Shi and Chen [24] provided better agreement with the experimentally determined liquid film diameter. The reason for this is mainly due to the fact that the correlation considers liquid fluid properties. It should be noted that these correlations do not predict breakup of the liquid film. Rather, the predicted film diameter was calculated up to the maximum film diameter.

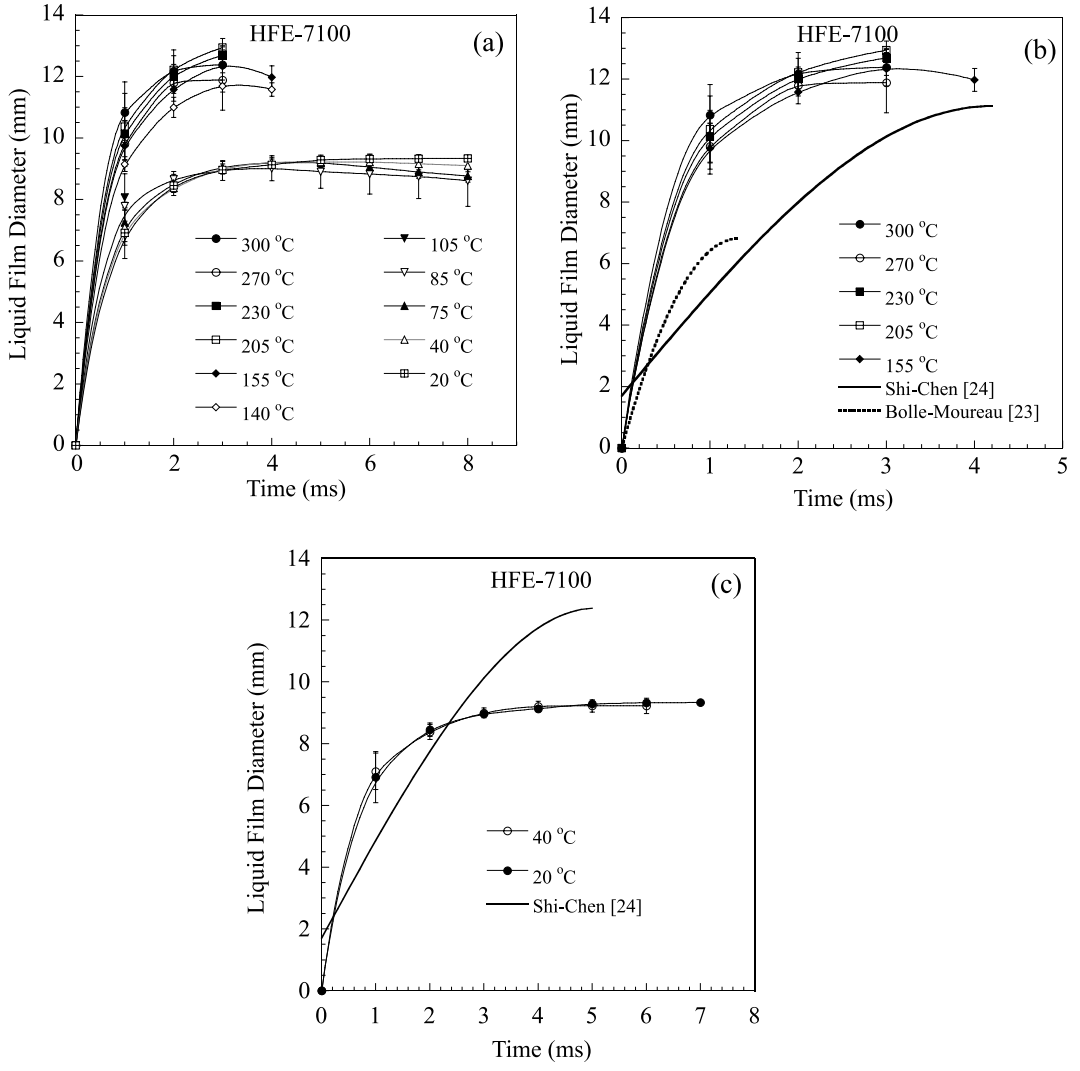

Fig. 4. (a) Measured liquid film diameter as a function of time for various temperatures for HFE-7100 for $We = 750$, (b) comparison of measured liquid film diameter with model results within the film boiling regime for HFE-7100, and (c) comparison of measured liquid film diameter with model results within the film evaporation regime for HFE-7100.

Shi and Chen [24] have proposed another correlation valid within the film evaporation regime. The correlation is given as:

$$D_{\mathrm{f}}(t) = 1.6V\left[t - (10^6 v)^{0.1}\frac{4\sigma V^{0.6}t^{2.95}}{\rho D^3}\right] + D \tag{5}$$

where v is the kinematic viscosity with the remaining variables the same as those defined in Eq. (4). Plotted in Fig. 4c is the measured and predicted liquid film diameter. For the film evaporation regime, the model over predicts the liquid film diameter. This is different than the under prediction of the liquid film diameter by various models within the film boiling regime. In addition, the correlation proposed by Kurokawa and Toda [25] was used to calculate the maximum film diameter for HFE-7100 impact at 20 °C in the film evaporation regime. The correlation is:

$$\frac{D_{\mathrm{f\,max}}}{D} = 0.96Re^{0.095}We^{0.084} \tag{6}$$

where D_{fmax} is the maximum film diameter, and Re the Reynolds number. The Reynolds number was defined as $Re = \rho VD/\mu$, where μ is the dynamic viscosity. The correlation is valid for $150 \leqslant We \leqslant 750$ and $850 \leqslant Re \leqslant 50{,}000$. The calculated maximum film diameter for HFE-7100 using this correlation is 6.7 mm. The measured value was 9.3 mm, a difference of 27%.

Based upon the discrepancies between the measured liquid film diameters and available model predictions for all regimes both boiling and non-boiling, it is clear that current correlations cannot be used to adequately describe HFE-7100 droplet impact. As discussed earlier, this result was expected since most correlations are valid for water impact.

Fig. 5 displays the measured evaporation lifetime as function of surface temperature for *n*-heptane droplets with an initial diameter of 3.0 ± 0.1 mm. Qualitatively, the curve is similar to HFE-7100. For surface temperature less than the normal boiling point of *n*-heptane, 98.4 °C, droplet impact should result in wetting of the impacted surface without boiling. The minimum evaporation time was observed to occur at 160 °C. Therefore, nucleate boiling is expected for surface temperatures from the boiling point, 98.5 °C, up to 160 °C. The Leidenfrost temperature for *n*-heptane was 210 °C. This is close to the value (205 °C) obtained by Chandra and Avedisian [14] for *n*-heptane on a stainless steel surface. Transition boiling will occur for *n*-heptane from 160 to 210 °C. Experiments were performed for *n*-heptane over the same boiling regimes for HFE-7100 impact, namely, 20 °C, 98.5 °C (boiling point), 160 °C (minimum evaporation time), 210 °C (Leidenfrost point), and 250 °C (film boiling).

Comparing the impact of *n*-heptane to HFE-7100 required matching the impact Weber number in addition to the boiling regimes. Matching the Weber number exactly is difficult since the Weber number is obtained from statistical averages of droplet diameter and impact velocity. The Weber number for *n*-heptane impact was equal to 714. The relative standard uncertainty in determining the Weber number was ±8%. Within experimental uncertainty, a Weber number of 714 may be considered similar to the Weber number of 750 for HFE-7100 impact. Fig. 6 displays *n*-heptane impact at $We = 714$ for surface temperatures of 20, 98, 160, 210 and 250 °C, respectively. Similar to HFE-7100 impact at the same temperature, the droplet was observed to spread and wet the surface. When compared to images obtained by Chandra and Avedisian [14] for *n*-heptane impact upon a solid metallic surface at 24 °C at Weber number equal to 43, the collision dynamics were qualitatively similar.

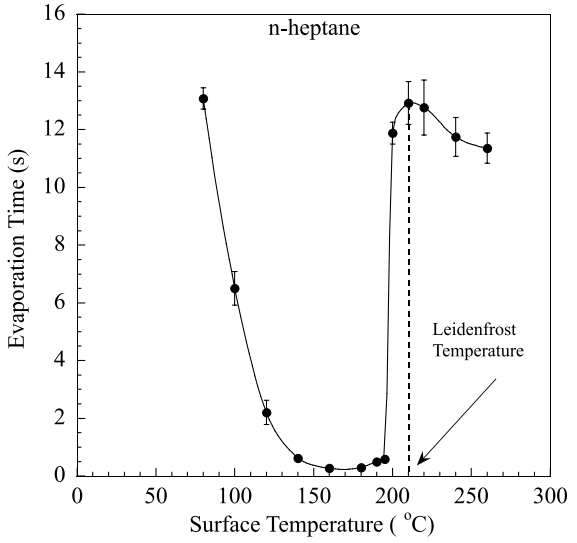

Fig. 5. Measured evaporation lifetime for *n*-heptane as a function of surface temperature.

For impact at 98 °C, the normal boiling temperature of *n*-heptane, the droplet was observed to spread, and at 4 ms after impact, cellular structures were observed to form within the liquid film. The cellular patterns observed for *n*-heptane by Chandra and Avedisian [14] are different than those in Fig. 6. The explanation could be due to the order of magnitude difference in the impact Weber number. The generation of cellular structures was qualitatively similar to HFE-7100 impact at 61 °C, the normal boiling point of HFE-7100. For *n*-heptane, however, these cellular structures resulted in a fingering phenomenon along the periphery of the liquid film diameter (see Fig. 6).

When the surface temperature was increased to 160 °C, the temperature of minimum evaporation time for *n*-heptane, differences were observed for *n*-heptane and HFE-7100 at their respective minimum evaporation temperatures. For HFE-7100 (see Fig. 3), immediately after impact, the droplet was observed to breakup into many small droplets. For *n*-heptane, however, the droplet did not breakup into many small droplets. Impact at 210 °C, the measured Leidenfrost temperature for *n*-heptane, resulted in similar collision dynamics to the impact at the Leidenfrost temperature of HFE-7100. Immediately after impact, the droplet was observed to flatten into a large disk. Small droplets were ejected from along the periphery of this disk. At 2 ms after impact, the small liquid film within the disk was observed to violently breakup into several droplets. Similarities between HFE-7100 and *n*-heptane were also observed within the film boiling regime (see Fig. 6) as well.

The spreading liquid film diameter as a function of time was measured for *n*-heptane and is displayed in Fig. 7a. The liquid film diameter was measured up to time of droplet breakup. The evolution of liquid film diameter for *n*-heptane displays differences compared to HFE-7100 (see Fig. 4a). The measured liquid film diameter for *n*-heptane is relatively independent of surface temperature. For HFE-7100 at film boiling, the liquid film diameter was considerably larger than film evaporation, nucleate boiling and the transition boiling regimes. For *n*-heptane, the film diameter was, within experimental uncertainty, the same magnitude as all other boiling

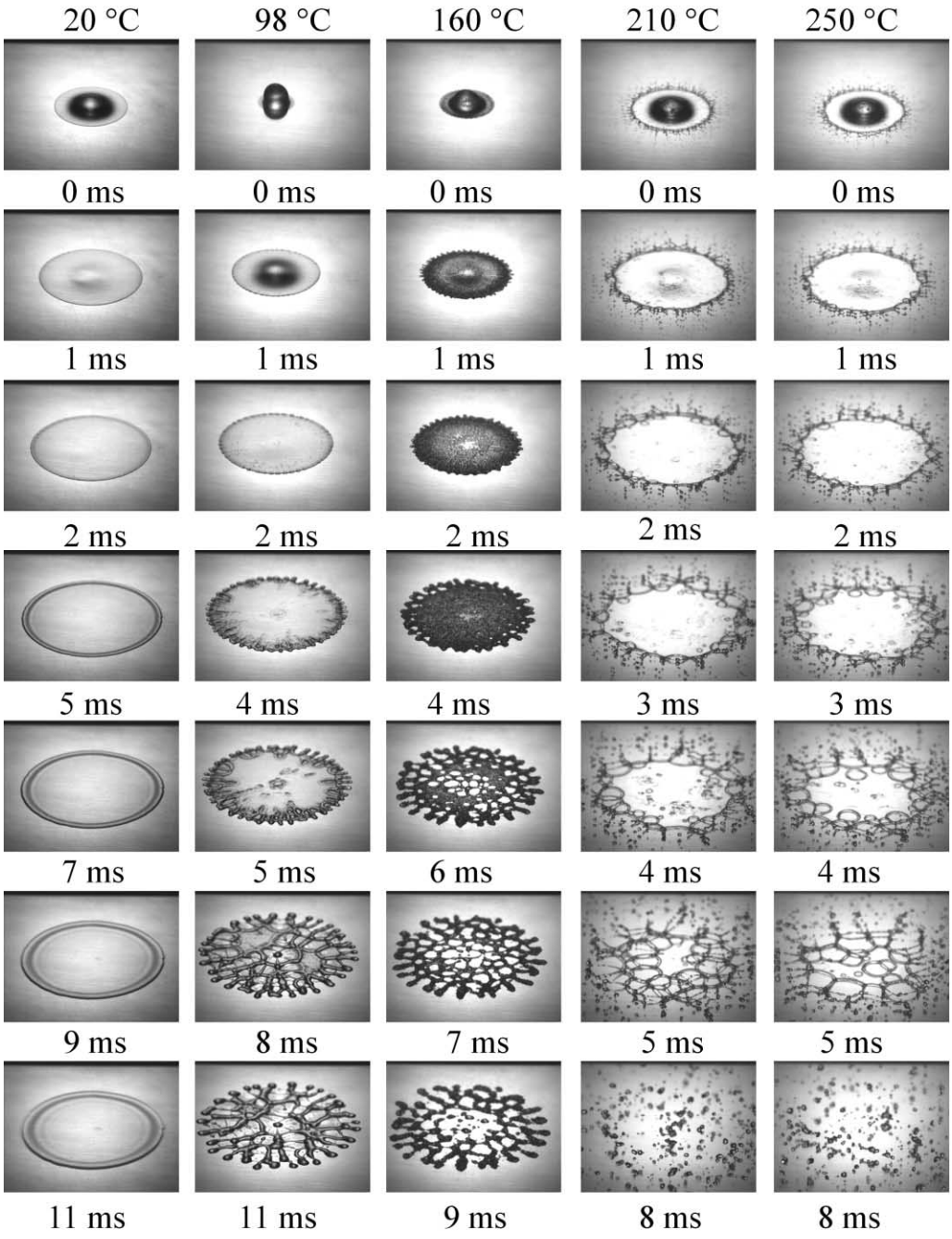

Fig. 6. Time elapsed images of *n*-heptane droplet impingement upon a stainless steel surface at $We = 714$.

regimes. Differences in the evolution of liquid film diameter for HFE-7100 and *n*-heptane within the film boiling regime were due to greater instability of the liquid film diameter for *n*-heptane. The liquid film diameter became unstable after 2 ms for *n*-heptane in the film boiling regime. The liquid film diameter was unstable as well within the nucleate boiling regime. The reason for this was the fingering phenomenon discussed earlier. Such patterns precluded further measurement of the liquid film diameter.

The measured evolution of liquid film diameter for *n*-heptane was compared to the experimental results of Chandra and Avedisian [14]. They observed the liquid film diameter to be independent of surface temperature

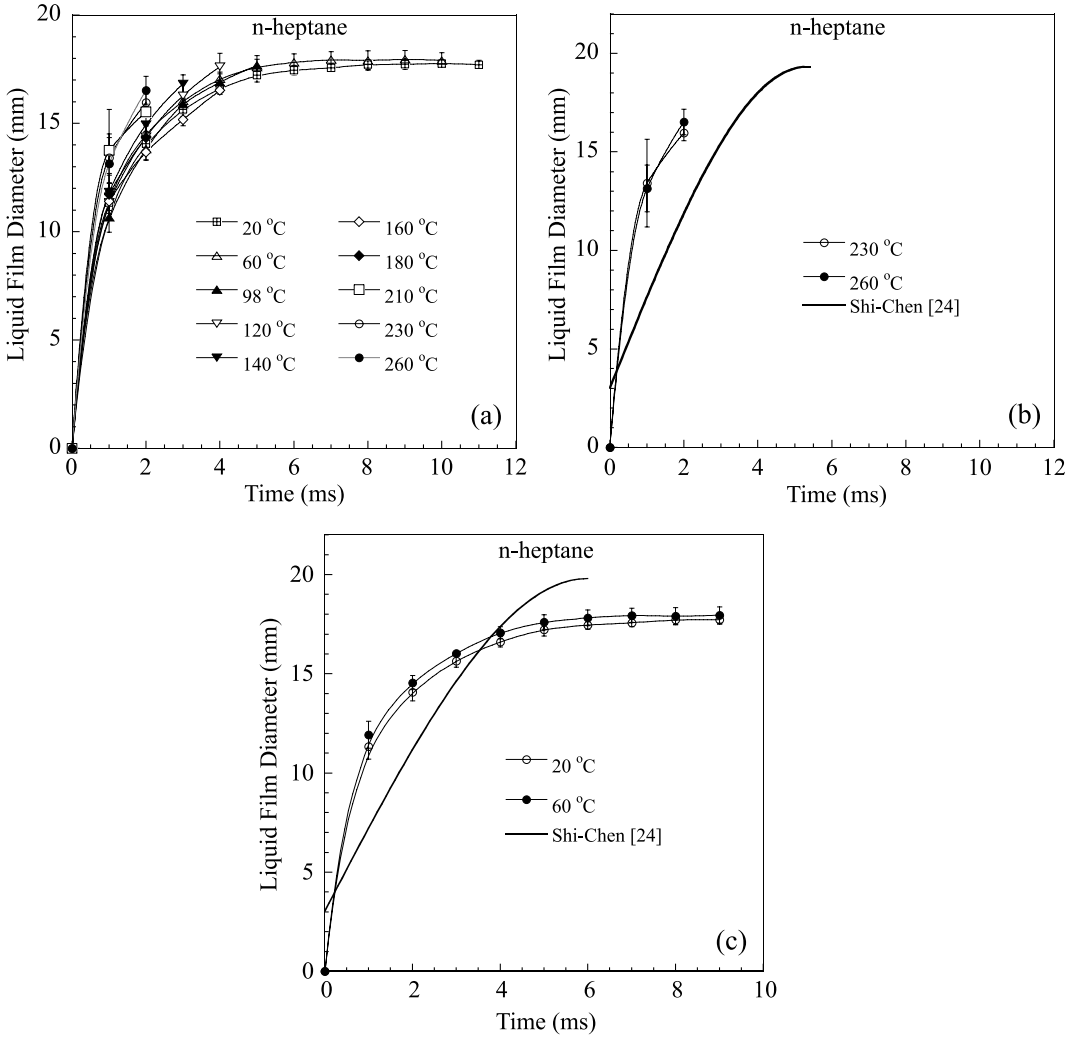

Fig. 7. (a) Measured liquid film diameter as a function of time for various temperatures for *n*-heptane for $We = 714$, (b) comparison of measured liquid film diameter with model results within the film boiling regime for *n*-heptane, and (c) comparison of measured liquid film diameter with model results within the film evaporation regime for *n*-heptane.

within the first 2 ms after impact. After the initial impact time, the maximum liquid film diameter decreased with increasing temperature. Such observations were not observed in Fig. 7a. Reasons for the difference are related to impact velocity, i.e. the impacting Weber number. For low Weber number impact investigated by Chandra and Avedisian [14], at sufficiently high surface temperature (film boiling regime), *n*-heptane droplets were observed to impact, recoil, and levitate above the surface. Droplet levitation occurred due to the pressure of the vapor between the solid surface and the droplet [14]. At the high impact Weber numbers used in the present study, the droplet spreads into a thin disk upon impact due to the high velocity impact. This thin disk then becomes unstable and breaks up into many tiny droplets. These tiny droplets are levitated upon the surface due the pressure of vapor blanket between the surface and droplet. Bernardin et al. [3] observed a qualitatively similar phenomenon for water droplet impact within the film boiling regime as the impact Weber number was increased from 60 to 220.

Model predictions discussed earlier were used to compare the spreading liquid film diameter of *n*-heptane. The correlation of Bolle–Moureau [23] also provided poor agreement to the experimental *n*-heptane data. Fig. 7b and c display the results of the correlation from Shi–Chen [24] for film boiling and film evaporation, respectively. Better agreement was realized for both the film evaporation and film boiling regimes for *n*-heptane than HFE-7100 with the Shi–Chen [24] correlations. How-

ever, these correlations are not able to predict liquid film breakup, thus these correlations cannot be used to represent impact at high Weber numbers.

4. Conclusions

This study has demonstrated that by knowing the evaporation curves for different fluids and matching the impact Weber number, the impact dynamics are qualitatively similar at different boiling regimes. While this allows for qualitative determination of the collision dynamics, it is insufficient for measurement of the liquid film diameter. The evolution of liquid film diameter with time is necessary to determine the portion of the surface undergoing surface cooling [3]. Thus, spreading characteristics of a particular fluid must be measured because current correlations describing the evolution of liquid film diameter with time are still lacking for high Weber number impact.

Acknowledgements

SLM acknowledges support from an NRC Post-Doctoral fellowship. A reviewer is acknowledged for providing comments invaluable to the integrity of the manuscript.

References

[1] M.D. King, J.C. Yang, W.S. Chien, W.L. Grosshandler, Evaporation of a small water droplet containing an additive, Proceedings of the ASME National Heat Transfer Conference, Baltimore, MD, 1997.
[2] B. Downie, C. Polymeropoulos, G. Gogos, Interaction of a water mist with a buoyant methane diffusion flame, Fire Safety J. 24 (1995) 359–381.
[3] J.D. Bernardin, C.J. Stebbins, I. Mudawar, Mapping of impact and heat transfer regimes of water drops impinging on a polished surface, Int. J. Heat Mass Transfer 40 (1997) 247–267.
[4] O. Reynolds, On the action of rain to calm the sea, Proc. Manchester Lit. Phil. Soc. 14 (1875) 7–14.
[5] O. Reynolds, On the floating of drops on the surface of water depending only on the purity of the surface, Proc. Manchester Lit. Phil. Soc. 21 (1881).
[6] J.W.S. Rayleigh, Further observations upon liquid jets, in continuation of those recorded in the Royal Society's Proceeding for March and May, 1879, Proc. R. Soc. London 34 (1882) 130–145.
[7] M. Rein, Phenomena of liquid droplet impact, Fluid Dyn. Res. 12 (1993) 61–93.
[8] O.G. Engel, Waterdrop collisions with solid surfaces, J. Res. NBS 5 (1955) 281–298.
[9] L.H.J. Wachters, N.A.Y. Westerling, The heat transfer from a hot wall to impinging water drops in the spheroidal state, Chem. Eng. Sci. 21 (1966) 1047–1056.
[10] F.P. Bowden, J.E. Field, The brittle fracture of solids by liquid impact, by solid impact and by shock, Proc. R. Soc. London A 282 (1964) 331–352.
[11] M.B. Lesser, Analytical solutions of liquid-drop impact problems, Proc. R. Soc. London A 377 (1981) 289–308.
[12] M.N. Al-Durrah, J.M. Bradford, Parameters for describing soil detachment due to single waterdrop impact, Soil Sci. Soc. Am. J. 46 (1982) 836–840.
[13] C.T Avedisian, J. Koplik, Leidenfrost boiling of methanol droplets on hot porous/ceramic surfaces, Int. J. Heat Mass Transfer 30 (1987) 1587–1603.
[14] S. Chandra, C.T. Avedisian, On the collision of a droplet with a solid surface, Proc. R. Soc. London A 432 (1991) 13–41.
[15] S. Chandra, C.T. Avedisian, Observations of droplet impingement on a ceramic porous surface, Int. J. Heat Mass Transfer 35 (1992) 2377–2388.
[16] Y.S. Ko, S.H. Chung, An experiment on the breakup of impinging droplets on a hot surface, Expt. Fluids 21 (1996) 118–123.
[17] R. Bola, S. Chandra, Parameters controlling solidification of molten wax droplets falling on a solid surface, J. Mater. Sci. 19 (1999) 4883–4894.
[18] S. Aziz, S. Chandra, Impact, recoil and splashing of molten metal droplets, Int. J. Heat Mass Transfer 43 (2000) 841–857.
[19] B.S. Kang, D.H. Lee, On the dynamic behavior of a liquid droplet impacting upon a inclined heated surface, Expt. Fluids. 29 (2000) 380–387.
[20] W.M. Pitts, J.C. Yang, M.L. Huber, L.G. Blevins, Characterization and identification of super-effective thermal fire extinguishing agents—First Annual Report, NISTIR 6414, US Department of Commerce, Washington DC, October 1999.
[21] Z. Tamura, Y. Tanasawa, Evaporation and combustion of a drop contacting with a hot surface, Proc. Combust. Inst. 7 (1959) 509–522.
[22] K.J. Baumeister, F.F. Simon, Leidenfrost temperature—it's correlation for liquid metals, cryogens, hydrocarbons, and water, J. Heat Transfer 95 (1973) 166–173.
[23] L. Bolle, J.C. Moureau, Spray cooling of hot surfaces, in: J.D. Hewitt, N. Zuber (Eds.), Multiphase Science and Technology, Hemisphere, New York, 1981, pp. 1–92.
[24] M.H. Shi, J.C. Chen, Behavior of a liquid droplet impinging on a solid surface, ASME 83-WA/HT-104, 1983.
[25] M. Kurokawa, S. Toda, in: J. Lloyd, Y. Kurosaki (Eds.), Proc. ASME/JSME Thermal Eng. Conf., vol. 2, 1991, pp. 141–146.